ELSEVIER

Journal of Chromatography A, 945 (2002) 103–115

JOURNAL OF CHROMATOGRAPHY A

www.elsevier.com/locate/chroma

Pore network modelling of the behaviour of a solute in chromatography media: transient and steady-state diffusion properties

L. Mattias Bryntesson[a,b,*]

[a]*Royal Institute of Technology, Department of Chemical Engineering and Technology, SE-100 44 Stockholm, Sweden*
[b]*Amersham Biosciences AB, Mattias Bryntesson, Bjorkgatan 30, SE-751 84 Uppsala, Sweden*

Received 7 November 2000; received in revised form 1 October 2001; accepted 6 November 2001

Abstract

A pore network model is presented, that is a geometrical simplification of a porous medium. The network consists of pore chambers interconnected by pore throats. A recursive algorithm for the simulation of mercury intrusion porosimetry in the network is presented. Calculations indicate that it is possible to fit simulated mercury intrusion data to experimental data, and thereby obtain parameters of the pore size distribution and pore topology (pore connectivity). A time-dependent material balance equation for diffusion on the pore level is set up and solved for the pore network. By calculating the concentration evolution in the network, the *transient diffusivity* and the *steady-state diffusivity* are found. When the network is well connected, those two diffusivities are equal, but for poorly-connected networks they differ. For migrating solutes that are non-negligibly small compared to the pore throats, considerable differences between the transient and steady-state diffusivities were found.

Keywords: Pore network model; Diffusion; Solute behaviour; Simulation; Porous media

1. Introduction

Porous materials often have complicated pore structures, with pores of different sizes and shapes, interconnected in different arrangements. The porous material can in some cases be well described as a pseudohomogeneous material, in which transport phenomena occur in a way similar to the way they would occur in a homogeneous material, that is the mathematics of the phenomena is similar. However, in order to obtain an understanding of how the pore structure affects the transport properties, a more detailed description of the material must be sought. Frequently, the pore structure is approximated by a model consisting of parallel pores with a distribution of sizes. Fitting such a model to experimental data would give one a pore size distribution that most often is different from the actual pore size distribution. For the case of mercury porosimetry, which has been analyzed by Lane [1], the intrusion of mercury gives information about the narrow necks of the pore structure, whereas the extrusion gives information about the size of the pore voids. Moreover, the measured pore sizes will deviate from the actual sizes because of network effects [1]. Current mercury porosimetry instruments employ the parallel

*Tel.: +46-18-612-0690; fax: +46-18-612-1844.
E-mail address: mattias.bryntesson@eu.amershambioscienes.com (L.M. Bryntesson).

0021-9673/02/$ – see front matter
PII: S0021-9673(01)01485-6

pore model which in general does not give the actual pore size distribution and internal surface area.

Much of the inadequacy of the parallel pore approximation can be intuitively grasped by considering the terms *shadowing* or *shielding*, having the meaning of large pores surrounded only by smaller pores. Mercury intruding into such a pore structure will intrude at the pressure corresponding to the smaller pores, but the intruded volume at that pressure will also include the volume of the larger pore. For a diffusion process, such a shielded pore will have high diffusional resistance for communication with the outer world, and it will have a large capacity for accumulating molecules. Another term that is self-explanatory, and that is used for pores consisting of a cavity with a narrow entrance opening, is *ink bottle* pores.

By describing a porous medium as a network of interconnected pores, a fairly general model is obtained, able to account for shielding. Selecting the sizes of the pores and the way they are interconnected, one obtains models for different materials. The network consists of *pore chambers* (sites, nodes or vertices) interconnected by *pore throats* (bonds, arcs or edges).

A model for transport phenomena in porous media thus could consist of: (1) the pore network and (2) models for the transport phenomena on the local (pore) level. Both parts are important, the local model providing the dynamic and equilibrium properties for each pore, and the network making it possible to calculate the *effective*, macroscopic, properties. A network model can in such a way be used in the modelling of transport processes such as single-phase and two-phase fluid flow, pore diffusion, sorption and capillary condensation [2–5].

When the solute size/pore size ratio is small and the concentration is low, ordinary pore diffusion occurs, whereas when the solute size is of the same order of magnitude as the pore size, one would expect size exclusion (molecular sieving) and restricted diffusion. Restricted or sterically hindered diffusion [6–11] is pore diffusion where the size of the diffusing molecule is of the same order of magnitude as the characteristic length of the pore structure, thus reducing the effective diffusivity (ultimately to zero, which happens at the percolation threshold). In their extended definition of restricted diffusion, Petropoulos et al. [11] also incorporate the effect of molecules adsorbing onto the pore walls hindering the subsequent transport through the pore. This means [11] that restricted diffusion may be a dynamic process, coupled with adsorption. Depending on local conditions, one or several of the mechanisms may have to be taken into account.

According to Zhang and Seaton [12], a pore network can get close to the percolation threshold if

- the network is poorly connected;
- the diffusing molecule has a size comparable to the pore size;
- the porous structure is multimodal, and the pores forming the largest mode are close to the percolation threshold.

Consider a network of connected pores having a size distribution and a solute whose size is somewhere in between the sizes of the largest and the smallest pore. Some of the pores will then be permeable to the solute molecules, whereas some pores will be impermeable. The permeable pores will then form pore clusters, possibly percolating the network. At the percolation threshold, such a cluster appears self-similar and it has been claimed (see e.g. Sahimi [13]) that such a percolating cluster is partially fractal, and thus diffusion on such a structure can be non-Fickian [14–17]. This can be understood by considering the many dead-end pores and branches of different sizes that are present. A diffusing molecule could expect to encounter many blind pores and clusters of pores, making the macroscopic motion slower than it would be in a continuum.

For a random walk in three dimensions we have [13]:

$$\langle \Delta x^2 \rangle = 6Dt \tag{1}$$

describing the movement of a diffusing particle. From that, Fick's first law:

$$J = -D\nabla c \tag{2}$$

that states that the molar flux J is proportional to the diffusivity D and to the concentration gradient ∇c, can be derived [18]. However, for disordered media that may not hold, and the diffusion can be non-Fickian [13] in the sense that it cannot be adequately modelled by Fick's first law using a constant value for the diffusivity. This can lead to large deviation in concentration profiles [19–21], and therefore it is

important to study both the dynamic and the steady-state mass transfer in such systems.

According to the above, a system with pore sizes of the same order of magnitude as the size of the solute of interest is more likely to be close to the percolation threshold than a pore system with larger pore sizes, providing the pore structures have the same topology. In, for example, adsorption in porous adsorbents, increasing the mean pore size of the porous medium can be expected to give faster mass transfer, but also a lower specific surface area and thus a lower equilibrium adsorption capacity. This trade-off between fast pore transport and high capacity (surface area) makes it possible that operating in the neighborhood of the percolation threshold may be optimal in some sense, and thus, the modelling of such systems is of interest. For porous media having diffusive transport through a bidisperse pore structure or media in which the transport is by both diffusion and convection [22] this could be applied for the regions of pores having sizes comparable to the size of the solute of interest. Imdakm and Sahimi [23], Petropoulos et al. [11] and Meyers and Liapis [24,25] have calculated transport properties for pore networks when the solutes have sizes comparable to the pore sizes.

It should be noted that the mapping of a porous medium onto a pore network is not unambiguous. For a stochastic material, a pore space skeleton can be found, e.g. using the method by Mohanty [3]. That method gives a primitive network topology with a constant connectivity of three which then has to be reduced to a working network. This reduction appears to be the crucial step, since it involves a change in topology, e.g. by collapsing groups of network elements into single elements (bonds or sites). The rules for such a collapse would involve some threshold value telling whether two nodes should be collapsed or not. This threshold rule will then affect the connectivity of the working network. As a consequence, for a pore network model, the connectivity can be expected to be strongly correlated with the pore sizes and the spatial correlation of the pore sizes.

1.1. Aims

We wish to develop a simulation tool that allows us to simulate the diffusive properties of the type of porous media that are used in chromatographic separations. Such a tool would be useful for selecting among different media to find the most appropriate for a specific application. It may also be useful for the design of such media.

1.2. Scope

The model is a pore network model and its properties are assumed to be obtainable primarily from mercury intrusion measurements. The work also sets out to find limitations in this approach and to indicate what additional observations may be useful or needed.

Firstly, the modelling of mercury porosimetry is described and some simulation results are shown. By adjusting the network model parameters, fitting of the mercury intrusion curve to experimental data could be done, and the porous material characterized in terms of the so estimated pore network parameters. Secondly, the diffusion model, including size exclusion, is formulated and solved for a few hypothetical cases. Size exclusion may be significant in chromatography applications with solutes, e.g. biomolecules, that are large compared to the pore sizes. This suggests a scheme for doing a priori calculations of transport properties of the porous medium.

2. Pore network generation

The network is defined by the local pore properties and by the network topology. All networks considered in this work are based on a cubic lattice with bonds connecting sites in an uncorrelated, random manner (a so-called bond-diluted network). This gives a variable connectivity (average coordination number). The maximum coordination number for a node in a cubic network is equal to six when one considers nearest neighbors only. Jerauld et al. [26] have shown that network conductivity mainly depends on the connectivity and not on the type of the underlying lattice and for any three-dimensional network the percolation threshold is reached at a connectivity of about 1.5 [27]. Therefore, in order to have higher connectivity in the model, it suffices to use the cubic lattice, with the extension that bonds may connect also second (and higher) nearest neighbors. Depending on the actual parameters, the lattice

may have to be considered as a ''distorted cubic'' lattice, since the node–node distances need not be constant. Similar mappings have been used previously [23–25].

The local pore properties could be defined in geometrical terms, e.g. as a network of sites, where each site is associated with a spherical pore, interconnected by bonds, associated with circular cylindrical pores. Another way would be not to express the network in such concrete terms, but instead let the pores be defined by e.g. their ''resistance'' or ''conductance'' for diffusion or the local *critical* pressure (which here is used for the pressure required for mercury penetration into an empty pore), and thus not specify a pore size distribution, but a distribution of conductances or critical pressures. The advantage with such an approach would be that properties that cannot directly be ascertained from a specific experiment would not be used when reporting results from such an experiment. Translating the conductance or pressure distribution to a pore size distribution would then be a separate task. The disadvantage would be that one usually has got some feeling for what the pore size distribution means, e.g. in terms of type of material or resulting properties, but the same feeling for a conductance or pressure distribution would have to be acquired. Also, one may have good reasons for using a specific functional form for the pore size distribution and assuming a specific pore geometry (from independent information such as direct observation of pore structure by microscopy or from knowledge about how the medium was formed). In that case, directly using the geometry would be a reasonable approach. In this paper, we will use simple geometric interpretations, and the nodes and bonds are defined as follows.

2.1. Pore throats (network bonds)

The pore throats are considered to be zero-volume connections between pore chambers and the diffusive transport rate of a very small molecule through one of the throats is given by

$$r = -D_{\mathrm{p}}^{i,j}\frac{\pi d_{\mathrm{t}}^2}{4}\frac{\Delta c}{\Delta x} \tag{3}$$

where $D_{\mathrm{p}}^{i,j}$ is the pore diffusivity, d_{t} is the pore throat diameter, Δc is the concentration difference between the two pore chambers connected to the throat and Δx is a characteristic length for the transport, which is taken here to be a function of the throat diameter. The exact geometrical interpretation of pore length could be the distance between two pore chambers.

In this work we have a pore throat diameter distribution (''pore size distribution'') which is generated by a pseudorandom number generator according to a predetermined distribution, The pseudorandom numbers are used for assigning values to the throat diameters, so that those are uncorrelated, i.e. the size of one throat is independent of the size of any other throat. Porous media may have polymodal and/or spatially correlated pore size distributions, that can also be handled by the model, but it is not considered in this work.

The pore size distribution is volume-based, and has a triangular frequency function with the mode m_v, the width to the left $\alpha_v m_v$ and to the right $\beta_v m_v$, i.e. the total width is $(\alpha_v + \beta_v)m_v$. The triangular distribution is physically unrealistic, but has the advantage of having a finite interval, outside which the probability is zero. Choosing a normal or log-normal distribution would be intuitively better, but then there is a need for truncating the distribution, since negative values are infeasible and there is a non-zero probability of getting very large values, unsuitable for calculations using finite networks. The triangular distribution does not have this shortcoming, and it makes it possible to create skewed distributions, as well as arbitrary distributions, by combining several triangles much in the same way as hat functions can be used to create piecewise linear function approximations. Nicholson and Petropoulos [28] used a set of similar simple distribution functions as models for pore size distributions. In order to use the volume-based distribution in the model, the distribution is first converted to a number-based distribution.

2.1.1. Pore shape

Often, it is reasonable to assume that the length of a throat is of the same order of magnitude as its diameter [5]. This assumes that the pores are somewhat ''compact'' and not like narrow cracks or slits.

However, from a geometrical perspective there should also be a dependence on connectivity, which can be exemplified as follows. Consider one of the bonds connected to a site. Depending on the total number of bonds connected to that site, each bond will have an upper limit on its size. The presence of many bonds would imply that the space around the site would have to be shared between those bonds, so that for the case of many bonds, they would have to be narrower (on an average) in order to fit in. The following approach is suggested in order to account for this:

- the connectivity, n_t, and the porosity ε, are known parameters, as well as the throat diameter, d_t, distribution;
- assign diameters from that distribution to the throats;
- one unit cell (pore chamber plus half of each connecting throat) is taken to have the sides equal to the length of a throat, l_t, and the volume thus becomes l_t^3;
- from the connectivity and the porosity, calculate the mode of the throat diameter/length ratio and use that over the whole network: $\varepsilon l_t^3 = (n_t/2)(l_t \pi d_t^2/4)$.

This will give a network with the desired porosity, and the pore length can be found from the resulting relation:

$$\frac{l_t}{d_t} = \sqrt{\frac{n_t \pi}{8\varepsilon}} \tag{4}$$

Strictly, since the above derivation is based on average values, the relation will not in general be valid for a pore size distribution, so the use of Eq. (4) for a pore size (and coordination number) distribution will be considered as a perturbation. Assuming constant pore sizes and coordination numbers throughout the network is a kind of effective medium theory (EMT) approximation [29,30]. Burganos and Sotirchos [31] used EMT and smooth field approximation to obtain the more accurate expression (as given by Friedman and Seaton [32]):

$$\frac{\langle l_t^2 \rangle}{\langle d_t^2 \rangle} = \frac{n_t \pi}{8\varepsilon} \tag{5}$$

EMT approximations have successfully been used for calculating network average properties, e.g. by Kirkpatrick [29] for resistor networks and by Nicholson and Petropoulos [33] and Petropoulos et al. [1] for transport in capillary networks.

It should be stressed that with knowledge about the actual pore structure, more effort should be put into finding reasonable relations between the model parameters, if that is possible. One could also imagine a scenario where pore diameter and length are uncorrelated or only weakly correlated.

2.2. Pore chambers (network nodes)

The pore chambers are considered to be perfectly mixed tanks, having a finite volume, derived from a given pore size distribution. When the network is constructed using a Monte Carlo technique, first the pore diameters $d_{t,i}$ are assigned to the throats. Then, the lengths $l_{t,i}$ are calculated from the values of $d_{t,i}$ and the connectivity n_t. Thereafter, the volume of the chamber is related to the diameters of the connecting throats through

$$V_c = \frac{1}{2} \sum_i \frac{\pi d_{t,i}^2}{4} l_{t,i} \tag{6}$$

i.e. it is equal to half of what would be the volume of the connecting throats if these were circular cylinders having diameters $d_{t,i}$ and lengths $l_{t,i}$.

At steady state, these assumptions are similar to the assumptions of zero-volumed chambers and straight, uniform pore throats, as used by Meyers and Liapis [24,25]. The two approaches are mathematically equivalent, but in this work both transient and steady-state situations are considered.

Our assumption about perfectly mixed pore chambers would be approximately satisfied as long as the characteristic times for diffusive mixing in the chambers is much smaller than the characteristic times for smoothing out concentration differences between adjacent chambers. Ideally, the assumption would be true for a network having very narrow throats connecting the chambers.

2.3. Network size and topology

To enable calculation of effective properties, the

network must be chosen sufficiently large, and in general, it should be (much) larger than the largest heterogeneities. However, for some purposes, the calculations can be done using smaller networks, and by averaging several calculations. The choice of network size will thus strongly depend on the type of material. As discussed above, for a network approaching the percolation threshold, the size of the heterogeneities approach infinity. This means that we can expect numerical difficulties in calculating effective properties for such a network. In Fig. 1 the importance of slab thickness for a mercury intrusion simulation is illustrated. The thicker the slab, the more pores are shadowed, and so the intrusion occurs at a higher pressure for thick slabs compared to thin ones. The intrusion curves could be smoothed by repeating the intrusion for another realization of the pore network and calculating the average intrusion curve. In practice, the relevant slab size can be found from simulation series such as the ones in Fig. 1 and the size is chosen where the effect is ''small enough'' in order to calculate the effective properties of a large sample. Here it should be noted that sometimes one may not be interested in the results for an infinite slab, but for a thinner slab, representing the finite geometry of the physical system. Again, more effort in this area should be made once the type of pore structure of the actual medium is identified and relevant assumptions can be made.

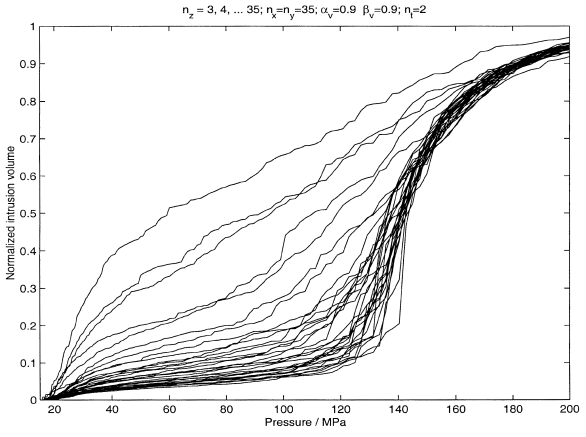

Fig. 1. Mercury intrusion into a porous slab with a connectivity of 2 and a pore size distribution with $m_v = 50$ nm, $\alpha_v = \beta_v = 0.9$. The slab size is $35 \times 35 \times n_z$, where n_z is varied from 3 (shallow curves) up to 35 (steep curves).

The geometry of the medium may also have to be accounted for by adjusting the pore topology, cf. the work by Meyers and Liapis [24,25] where the network includes, apart from an intraparticle pore cluster, an irregular ''interstitial'' cluster which accounts for particle shape and boundary conditions for diffusion and convection inside the particle in the fixed bed.

3. Mercury porosimetry

Mercury porosimetry is a way of obtaining information about the pore structure of a material. The sample is evacuated using a vacuum and placed in liquid mercury. Pressure is increased, and due to the fact that mercury does not wet most samples, it will not go into a pore until the pressure is equal to or larger than the capillary pressure corresponding to that pore size.

Usually some form of the Washburn [34] equation is used:

$$P = \frac{4\gamma \cos\theta}{d} \tag{7}$$

where γ is the surface tension at the meniscus, d is the pore diameter (assuming circular cylindrical pores) and θ is the contact angle between the mercury and the pore wall.

The experimental pressure–volume values are then usually interpreted by applying the equation to the recorded pressure, giving a pore size distribution, thus implicitly assuming a model with parallel capillaries. However, often such a model is a rough simplification of the actual pore structure [5]. The use of a pore network is an important step towards more realistic models. Lane [1] has investigated mercury porosimetry with a pore network model, and Loh [35] and Meyers [36] have used pore network models for characterizing chromatography media.

The network used here for mercury intrusion is a rectangular, three-dimensional slab, with one side exposed to the external mercury source. The opposite side is closed, thus introducing a local change in pore connectivity, so it is important to select the size of the network sufficiently large not to let this change unintentionally influence the result. The number of model pores in this direction could be

thought of as a characteristic depth of the model porous medium, and could correspond to the particle radius for a porous particle, or the distance between macropores [37] in a particle with a bidisperse pore size distribution. The remaining four sides have natural (periodic) boundary conditions.

From a macroscopic point of view, the relationship measured is a pressure–volume curve. Also on the pore level there is a pressure–volume relationship, e.g. according to the Washburn equation (Eq. (7)). For a straight, circular cylindrical pore, the relationship is a rectangular function, with zero intrusion volume until the point where pressure is high enough according to Eq. (7) (the ''critical'' pressure) and at that point it is completely filled. For conical pores, the pressure–volume curve will depend on the direction in which the pore is filled. From the narrow end it will be rectangular, since any mercury coming in will be able to fill the whole pore. From the wide end, it will be a continuous function, modelling that the pore will be filled over a range of pressures.

For the case of rectangular pore pressure–volume curve, we need only to record whether or not a pore is filled. The nature of the intrusion process lends itself to a recursive modelling approach, and the algorithm works by tracking the continuous path of mercury from the outside surface and into the pore network. When a meniscus which is a candidate for expansion is found, it is tested by comparing the current pressure and the critical pressure for the pore which is a candidate for being filled. If a pore gets filled (or already was filled) its menisci are tested likewise, otherwise that branch is exhausted and the ''tracker'' can safely jump up one recursive level. The process of intrusion makes the recursive approach intuitively appealing, and there is need for one single scan per pressure, compared to an iterative program like that of Loh [35], where the network must be scanned several times for each pressure point until no change occurs.

4. Mercury intrusion simulation results

Mercury intrusion was simulated for a reference case which was then perturbed (Fig. 2). The resulting curve family shows that changing the parameters gives rise to differently shaped curves. This indicates that the simultaneous estimation of the network parameters is possible by fitting the calculated curve to experimental data. The effect of connectivity seems to be relatively weak, though, so it would be beneficial if one could get an independent estimate from e.g. microscopy.

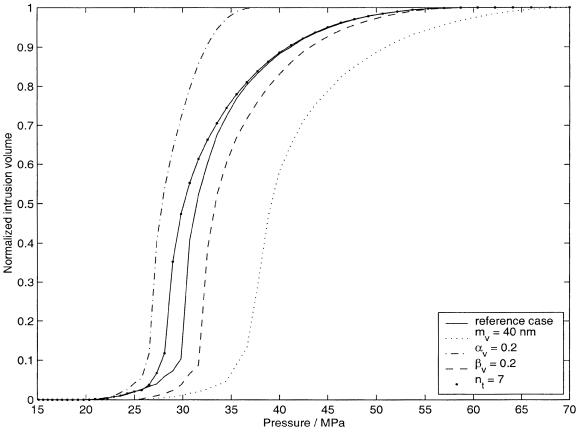

Fig. 2. Calculated cumulative mercury intrusion volume versus applied pressure. The parameter values for the reference case are: $m_v =$ 50 nm, $\alpha_v = \beta_v =$ 0.5 and $n_T =$ 5. By perturbing one parameter at a time, with the values given in the figure, it is observed that the intrusion curve varies in different ways depending on the parameter perturbed. That indicates that it could be possible to determine unique parameter values when fitting the model curve to experimental data.

5. Transient and steady-state diffusion in the network model

Loh [35], Loh and Wang [38] and Meyers [36] have studied size exclusion in their network models, by calculating accessible volume for a given solute size. Meyers and Liapis [24,25] and Meyers [36] have calculated the convection and diffusion for both small and large molecules under unretained as well as adsorbing conditions in a pore network at steady state. Here, the transient and steady-state diffusion of small and large molecules in a network is studied. The molecular diffusivity is assumed constant and the molecules are unretained. The driving force for diffusion is the concentration difference between connected pore chambers. Size exclusion effects are

accounted for, and the following assumptions are also made:

- the pore chambers hold all of the pore volume;
- the resistance to mass transfer lies in the pore throats.

This is equivalent to saying that the pore chambers can be considered as perfectly stirred tanks, and that the mass transfer between tanks occur through zero-volume pipes between connected tanks. The mass flux is proportional to the pore diffusivity, to the throat cross-section area, and to the difference between the concentrations of the connected chambers.

Since the network consists of discrete pores, the corresponding model is also discrete. The material balance for a pore chamber can be written as

$$V_c^i \frac{dc^i}{dt} = \sum_j D_p^{i,j} A^{i,j} \frac{(c^j - c^i)}{\Delta x^{i,j}} \tag{8}$$

where the superscript i denotes a chamber according to some numbering system and V_c^i is the volume of that chamber. $A^{i,j}$ denotes the cross-sectional area of the throat connecting chambers i and j, c^i and c^j are the chamber concentrations and $\Delta x^{i,j}$ is the corresponding chamber–chamber distance or throat length, which is taken to be the characteristic length for the concentration gradient. The summation is thus carried out over all throats j connected to the chamber i. Eq. (8) at steady state is similar to the approach by Meyers and Liapis [24].

Defining a conductance matrix E with off-diagonal elements:

$$E_{i,j} = \frac{D_p^{i,j} A^{i,j}}{V_c^i \, \Delta x^{i,j}} \tag{9}$$

and the diagonal elements defined by

$$E_{i,i} = -\sum_{j \neq i} E_{i,j} \tag{10}$$

we get

$$\frac{dc}{dt} = Ec \tag{11}$$

with the vector c with all chamber concentrations.

In order to account for steric hindrance effects, the pore diffusivity is defined by

$$D_p^{i,j} = \alpha^{i,j} D_m \tag{12}$$

where $\alpha^{i,j}$ is a geometric hindrance factor based on the molecule size and pore size and shape. For a spherical molecule in a circular cylinder the equation

$$\alpha^{i,j} = (1 - \lambda^{i,j})^4 \tag{13}$$

is used, where $\lambda^{i,j} = d_{sol}/d_t^{i,j}$ is the ratio of the molecule diameter d_{sol} to the diameter $d_t^{i,j}$ of the throat between chambers i and j. It is equivalent to the equation of Spry and Sawyer [9] as used by Zhang and Seaton [12], and it follows closely the relation due to Renkin [6]:

$$\alpha^{i,j} = (1 - \lambda^{i,j})^2 (1 - 2.104\lambda^{i,j} + 2.089(\lambda^{i,j})^3 - 0.948(\lambda^{i,j})^5) \tag{14}$$

The molecular diffusivity is estimated using the Stokes–Einstein equation:

$$D_m = \frac{kT}{3\pi\mu d_{sol}} \tag{15}$$

In order to evaluate the properties of the network, the following numerical experiment is carried out. Typical boundary and initial conditions are:

- Initial concentration of zero everywhere.
- One side of the rectangular 3D slab network is exposed to a finite, constant, non-zero concentration c_0 starting at $t = 0$.
- The concentration in the pores at the opposite side of the slab is held at zero.
- The remaining four sides have periodic boundary conditions, meaning that a mass flow through a throat pointing outwards comes in again through an identical throat on the opposite side. This condition introduces a local correlation of length equal to the slab dimensions in those directions.

Those conditions mean that we have an empty network, which we expose with a concentration step, and we follow the concentration evolution over time. From this concentration evolution $c(x_i, y_j, z_k, t)$ we calculate an average concentration profile:

$$c_{avg}(z_k, t) = \frac{\sum_{i=1}^{n_x} \sum_{j=1}^{n_y} c(x_i, y_j, z_k, t) \, V_c(x_i, y_j, z_k, t)}{\sum_{i=1}^{n_x} \sum_{j=1}^{n_y} V_c(x_i, y_j, z_k, t)} \tag{16}$$

For natural reasons, this sum will approach a steady-state solution as $t \to \infty$.

The applied concentration step constitutes an input step to the model and the output is the resulting concentration profile and the flux through the slab. The advantage of using a step is that both a transient response and a steady-state solution are obtained. The choices of conditions should not be considered as an attempt to model the actual physics, but is a simple computational experiment in order to identify the dynamic and steady-state properties of the network.

By choosing the network sufficiently large, *effective medium properties* can be found. The network size must then be much larger than the heterogeneties (e.g. due to varying pore sizes). Note that the calculations have been done for an unretained solute. One way of interpreting the results would be to calculate an effective diffusivity for the network.

This has been done in two ways:

- By calculating it using a version of Ficks' first law for the steady-state profile

$$D_{ss} = \frac{J\,\Delta z}{\Delta c} \tag{17}$$

where D_{ss} is the effective diffusivity, $J > 0$ the flux through the network at steady-state, Δz is the thickness of the slab and Δc the concentration difference over the network in the z-direction.

- By comparing the time to reach e.g. steady state with a profile calculated with a known (effective) diffusivity. Fourier's number is the quantity which characterizes a process like this, and by defining the fractional steady state to be reached at a time t_{fss} for a network or slab of thickness Δz and a *transient diffusivity* of D_{tr}:

$$\mathrm{Fo} = \frac{D_{tr}\,t_{fss}}{(\Delta z)^2} \tag{18}$$

If this is to be compared to a reference case with the corresponding variables t_{ref}, Δz_{ref} and D_{ref}, we get

$$D_{tr} = D_{ref}\,\frac{t_{ref}}{t_{fss}}\,\frac{(\Delta z)^2}{(\Delta z_{ref})^2} \tag{19}$$

Typically, D_{tr} is calculated at a number of t_{fss}, and the median is reported, in order to avoid possible outliers.

These effective diffusivities D_{ss} and D_{tr} may or may not be equal. For homogeneous media and for networks with high connectivity they are equal, but for networks having low connectivities they differ, which indicates that the diffusion is non-Fickian as mentioned above. Taking restricted diffusion into account, this can be a local effect, and possibly not easily distinguished from other simultaneously occurring phenomena.

5.1. Comparison with finite differences

The model for heterogeneous media should be able to handle homogeneous media as a special case, and the above network formulation is indeed capable of that. Consider a discretization in space of Ficks second law for a pseudohomogeneous medium with the effective diffusivity D_{eff}:

$$\frac{\partial c}{\partial t} = D_{eff}\nabla^2 c \tag{20}$$

using finite differences on a equidistant ($\Delta x = \Delta y = \Delta z = h$) cubic grid. We use Cartesian coordinates for which

$$\nabla^2 c(x, y, z, t) = \frac{\partial^2 c}{\partial x^2} + \frac{\partial^2 c}{\partial y^2} + \frac{\partial^2 c}{\partial z^2} \tag{21}$$

Using second-order difference approximations we get

$$\begin{aligned}\nabla^2 c(x, y, z, t)h^2 \approx\ & c(x + h, y, z, t) - 2c(x, y, z, t) \\ & + c(x - h, y, z, t) \\ & c(x, y + h, z, t) - 2c(x, y, z, t) + c(x, y - h, z, t) \\ & c(x, y, z + h, t) - 2c(x, y, z, t) + c(x, y, z - h, t) \\ =\ & \sum_{j=1}^{6}(c^j - c)\end{aligned} \tag{22}$$

where the index j could denote the throats around a chamber in a pore network (cf. Eq. (8)). That is, one obtains the same discretization as for the pore network model used here, if it is simplified to the same geometry.

5.2. Calculation of transient diffusivity

If the model slab is truly homogeneous, the problem is simplified to one space dimension, due to symmetry. Scaling the variables with the slab size Δz, some characteristic time Δt and the concentration step c_0, we get

$$\begin{aligned} Z &= z/\Delta z \\ T &= t/\Delta t \\ C &= c/c_0 \end{aligned} \tag{23}$$

and the equation becomes

$$\frac{\partial C}{\partial T} = \mathrm{Fo}\nabla^2 C = \mathrm{Fo}\frac{\partial^2 C}{\partial Z^2} \tag{24}$$

and the Fourier number defined by

$$\mathrm{Fo} = \frac{D\,\Delta t}{(\Delta z)^2} \tag{25}$$

the above boundary and initial conditions become

$$\begin{aligned} &C(Z, T=0) = 0 \quad 0 \le Z \le 1 \\ &C(Z=0, T) = 1 \quad T > 0 \\ &C(Z=1, T) = 0 \quad T > 0 \end{aligned} \tag{26}$$

which can be solved (see e.g. Crank [21] or Carslaw and Jaeger [39]) to give

$$C(Z, T) = 1 - Z - \sum_{i=1}^{\infty} \frac{2}{i\pi} \exp(-i^2\pi^2 \mathrm{Fo}\, T) \sin(i\pi Z) \tag{27}$$

This solution is suitable for finding t_{ref} in Eq. (19).

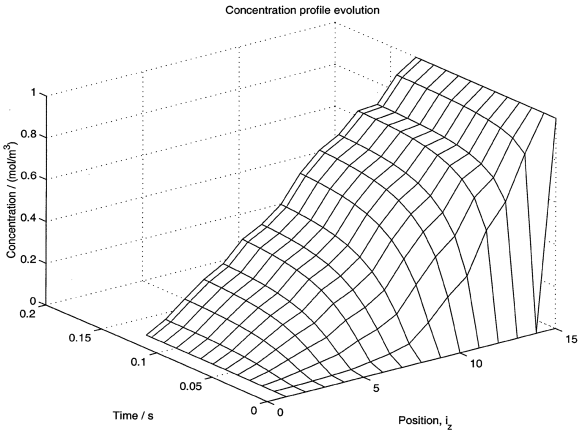

Fig. 3. Average concentration profile evolution in the slab.

6. Diffusion simulation results

In Fig. 3, the average concentration profile evolution in the slab is shown. The transport rate into and out from the slab are plotted in Fig. 4.

The connectivity and solute size was varied, and the other conditions for the simulations are:

Parameter	Value
m_v, throat diameter (nm; volume mode)	50
α_v, left distribution parameter	0.5
β_v, right distribution parameter	0.5
ε, porosity	0.7

Figs. 5 and 6 show steady-state diffusivity and the ratio between steady-state and transient diffusivities for various connectivities and molecule sizes. The diffusivities are normalized by the estimated free molecular diffusivity. The data are somewhat uncertain, especially close to the percolation threshold, because at the threshold, the size of the heterogeneties approach infinity, and thus a finite network cannot be expected to give good effective properties. However, it is clear that for low values of the connectivity, the ratio of steady-state to transient diffusivity is very low, indicating non-Fickian diffusion in the sense mentioned above. At high values of the connectivity (well-connected networks) the ratio approaches the value of the network porosity for

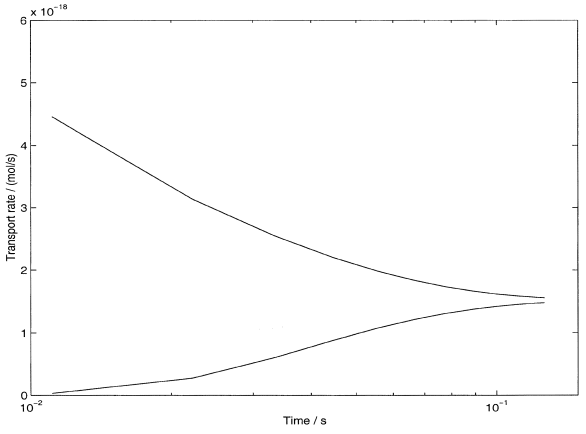

Fig. 4. Transport rate in (top) and out (bottom) of slab versus time.

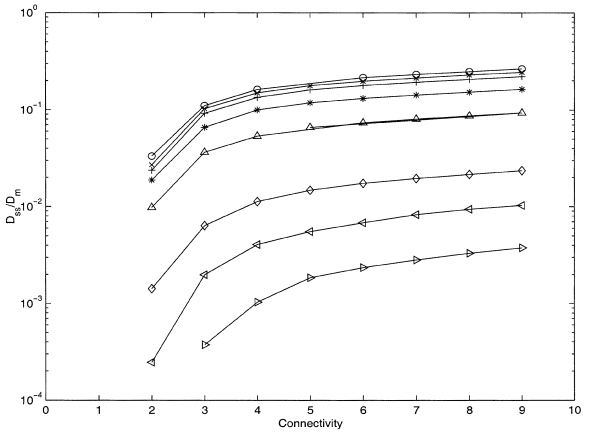

Fig. 5. Simulated steady-state diffusivity relative to molecular diffusivity as a function of pore connectivity. Solute sizes are 0.1 nm (○), 1 nm (×), 2 nm (+), 5 nm (★), 10 nm (△), 20 nm (◇), 25 nm (◁) and 30 nm (▷).

small solutes, and a lower value for larger solutes, reflecting that large solutes do not have access to all of the pore space. Also, the percolation threshold is a function of pore structure and molecule size, which is seen by the fact that the steady-state diffusivity approaches zero at low connectivities, and the larger the molecule is, the higher must be the connectivity in order to allow for transport through the material. This can be understood by considering the number of pore throats that the solute is able to penetrate. If the solute can penetrate 50% (number) of the throats, the

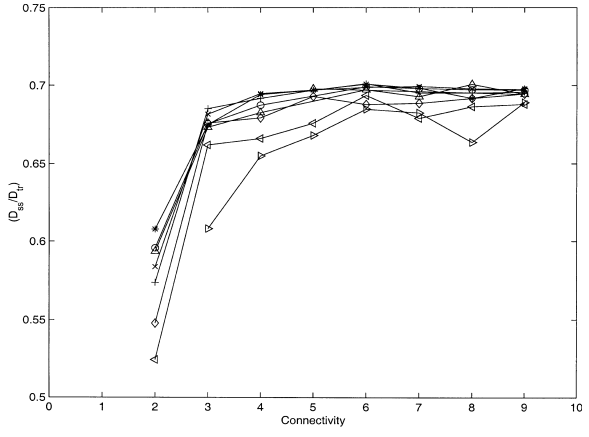

Fig. 6. Ratio between steady-state and transient diffusivity as a function of pore connectivity. Symbols as in Fig. 5.

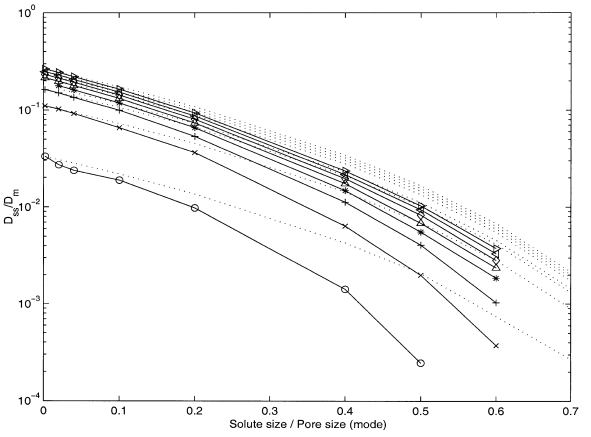

Fig. 7. Normalized steady-state diffusivity as a function of solute size to pore size ratio for various pore connectivities. The mode of the pore diameter is taken to be the characteristic pore size. $n_t = 2$ (○), 3 (×), 4 (+), 5 (★), 6 (△), 7 (◇), 8 (◁) and 9 (▷). The dotted curves represent solute size dependence according to Eq. (13).

threshold connectivity doubles (from 1.5 to 3) for uncorrelated pore sizes.

Moreover, the influence of hindrance (Eq. (13)) is significant already when the molecule size is of an order of magnitude smaller than the pore.

In Fig. 7, the steady-state diffusivity is plotted against solute size with the connectivity as a parameter. The diffusivity is normalized by dividing it by the free molecular diffusivity, since that is a function of solute size. The solute size is expressed in relation to the mode of the pore throat diameter. The dependence of solute size on pore diffusivity as given by Eq. (13) is indicated by dotted lines. This means that the network effects are somewhat isolated, and the degree of deviation from the dotted lines can be regarded as a network effect, or ''tortuosity'', loosely speaking. It is noted that the influence seems to be strongest for the lowest connectivity and that the curves with high connectivities represent networks where the heterogeneties are due to pore size distribution only, and not due to network topology.

7. Conclusions

A set of tools for doing a priori calculations of

effective diffusivity in porous media has been presented.

If a pore network representing the pore structure is known, the diffusivity can be found using a diffusion model together with the network model, and transient and steady-state diffusivities can be calculated.

For the more realistic case when the pore structure is unknown, a model for mercury intrusion together with the network model can be used for estimating the network parameters. However, additional data such as micrographs, if available, should be used in order to be able to make reasonable assumptions about the pore structure. An important observation made from the model studies was that the pore connectivity influences the mercury intrusion curve only weakly if the pore size distribution is narrow. The parameters m_v, α_v, β_v and n_t influence the intrusion curves in distinct ways, so the estimation of those parameters from experimental data seems possible taking into account the above.

The transient and steady-state effective diffusivities were calculated using the pore network. Close to the percolation threshold the transient diffusivity to steady-state diffusivity ratio diverges, and this can be explained by the fact that the pores accessible for transport form a fractal. For molecules smaller than the smallest pore in the network, percolation threshold is at a connectivity of about 1.5. For larger molecules, where only some fraction of the network is accessible, the threshold is shifted up towards higher connectivity so that the set of accessible pores has a connectivity of about 1.5.

The simulations show clearly that the diffusive properties of the network quickly deteriorate when the connectivity decreases. Then the non-Fickian behaviour becomes evident and the diffusivity drops markedly. It would thus be advantageous to design media with a not too low connectivity. Moreover, the phenomena observed with the present diffusion model cannot be modelled using Fick's law with a constant effective diffusivity.

8. Nomenclature

$A^{i,j}$	throat cross-area between chambers i and j	m^2
c	concentration	mol/m^3
c^i, c^j	concentration in chamber i, j	mol/m^3
c_{avg}	average concentration for a slice of the network	mol/m^3
Δc	concentration difference across slab	mol/m^3
C	dimensionless concentration	–
d	diameter	m
d_{sol}	diameter of a spherical solute	m
d_t	pore throat diameter	m
$d_t^{i,j}$	pore throat diameter between chambers i and j	m
D	diffusivity	m^2/s
D_m	free molecular diffusivity	m^2/s
D_p	pore diffusivity	m^2/s
D_{ref}	reference diffusivity	m^2/s
D_{ss}	steady-state diffusivity	m^2/s
D_{tr}	transient diffusivity	m^2/s
E	conductance matrix	$1/s$
Fo	Fourier number	–
h	finite difference discretization length	m
i, j	pore chamber number	–
J	molar flux	$mol/m^2\,s$
k	the Boltzmann constant $\approx 1.38066 \times 10^{-23}$	J/K
l_t	pore throat length	m
m_v	volume-based mode of pore size distribution	m
n_t	pore connectivity	–
P	pressure	Pa
r	transport rate	mol/s
t	time	s
t_{ref}	reference characteristic time	s
t_{fss}	characteristic time until fractional steady state	s
T	dimensionless time	–
T	temperature	K
V_c^i	volume of chamber i	m^3
x	spatial coordinate	m
$\Delta x^{i,j}$	characteristic length between chambers i and j	m
$\langle x^2 \rangle$	mean square distance	m^2
Δz	slab thickness	m
Δz_{ref}	reference slab thickness	m
Z	dimensionless spatial coordinate	–
α_v	left pore size distribution parameter	–
$\alpha^{i,j}$	hindrance factor between chambers i and j	–

β_v	right pore size distribution parameter	–
γ	surface tension	N/m
ε	porosity	–
θ	contact angle between mercury and pore wall	rad
$\lambda^{i,j}$	$d_{sol}/d_t^{i,j}$	–
μ	dynamic viscosity	Pa s
$\langle \cdot \rangle$	expectation value	

Acknowledgements

This work was in part carried out within the Centre for Bioprocess Technology at the Royal Institute of Technology (KTH), Stockholm, Sweden. Financial support from Amersham Biosciences AB is gratefully acknowledged. For help and discussions I would like to thank Professor I. Neretnieks, KTH, Dr L. Hagel and Dr K. Lacki, Amersham Biosciences AB, Uppsala, Sweden, and Professor A.I. Liapis, Dr J.J. Meyers and B.A. Grimes, University of Missouri–Rolla, USA.

References

[1] A.M. Lane, Interpretation of Mercury Porosimetry Data, Ph.D. thesis, University of Massachusetts, 1984.
[2] I. Fatt, Trans. AIME 207 (1956) 144.
[3] K.K. Mohanty, Fluids in Porous Media: Two-Phase Distribution and Flow, Ph.D. thesis, University of Minnesota, 1981.
[4] J.H. Petropoulos, J.K. Petrou, A.I. Liapis, Ind. Eng. Chem. Res. 29 (1991) 1281.
[5] F.A.L. Dullien, Porous, Media — Fluid Transport and Pore Structure, 2nd ed., Academic Press, New York, 1992.
[6] E.M. Renkin, J. Gen. Physiol. 38 (1954) 225.
[7] G.K. Ackers, R.L. Steere, Biochim. Biophys. Acta 59 (1962) 137.
[8] J.L. Anderson, J.A. Quin, Biophys. J. 14 (1974) 130.
[9] J.C. Spry, Jr., W.H. Sawyer, Paper 30C, 68th Annual AIChE Meeting, Los Angeles, Nov. 16–20, 1975.
[10] W.M. Deen AIC, AIChE J. 33 (1987) 1409.
[11] J.H. Petropoulos, A.I. Liapis, N.P. Kolliopoulos, N.K. Kanellopoulos, Bioseparation 1 (1990) 69.
[12] L. Zhang, N.A. Seaton, AIChE J. 38 (1992) 1816.
[13] M. Sahimi, Flow and Transport in Porous Media and Fractured Rock, VCH, Weinheim, 1995.
[14] D. Ben-Avraham, S. Havlin, J. Phys. A Math. Gen. 15 (1982) L691.
[15] S. Havlin, D. Ben-Avraham, H. Sompolinksy, Phys. Rev. A 27 (3) (1983) 1730.
[16] S. Havlin, D. Ben-Avraham, Adv. Phys. 36 (6) (1987) 695.
[17] Y. Gefen, A. Aharony, S. Alexander, Phys. Rev. Lett. 50 (1) (1983) 77.
[18] P.A. Egelstaff, An Introduction to the Liquid State, Oxford University Press, 1992.
[19] P. Neogi, Diffusion in Polymers, Marcel Dekker, New York, 1996.
[20] E. Guyon, C.D. Mitescu, J.-P. Hulin, S. Roux, Physica D 38 (1989) 172.
[21] J. Crank, The Mathematics of Diffusion, 2nd ed., Oxford University Press, 1975.
[22] N.B. Afeyan, N.F. Gordon, I. Mazsaroff, L. Varady, S.P. Fulton, Y.B. Yang, F.E. Regnier, J. Chromatogr. 519 (1990) 1.
[23] A.O. Imdakm, M. Sahimi, Phys. Rev. A 36 (11) (1987) 5304.
[24] J.J. Meyers, A.I. Liapis, J. Chromatogr. A 827 (1998) 197.
[25] J.J. Meyers, A.I. Liapis, J. Chromatogr. A 852 (1999) 3.
[26] G.R. Jerauld, L.E. Scriven, H.T. Davis, J. Phys. C 17 (1984) 3429.
[27] V.P. Zhdanov, Adv. Catal. 39 (1993) 1.
[28] D. Nicholson, J.H. Petropoulos, J. Phys. D 6 (1973) 1737.
[29] S. Kirkpatrick, Phys. Rev. Lett. 27 (25) (1971) 1722.
[30] A.I. Liapis, personal communication, 2000.
[31] V.N. Burganos, S.V. Sotirchos, AIChE J. 33 (1987) 1678.
[32] S.P. Friedman, N.A. Seaton, Chem. Eng. Sci. 50 (1995) 897.
[33] D. Nicholson, J.H. Petropoulos, J. Phys. D 10 (1977) 1911.
[34] E.W. Washburn, Proc. Natl. Acad. Sci. 7 (1921) 115.
[35] K.-C. Loh, A network model for perfusion chromatography, Ph.D. thesis, Massachusetts Institute of Technology, 1995.
[36] J.J. Meyers, Network Modeling of the Pore Structure of Porous Media for Determining the Diffusion and Convective Flow of a Solute in Monoliths and Columns packed with Chromatographic Particles, Ph.D. thesis, University of Missouri–Rolla, 2000.
[37] N.A. Seaton, Chem. Eng. Sci. 46 (8) (1991) 1895.
[38] K.-C. Loh, D.I.C. Wang, J. Chromatogr. A 718 (1995) 239.
[39] H.S. Carslaw, J.C. Jaeger, Conduction of Heat in Solids, 2nd ed., Oxford University Press, 1959.